

RESULTS FROM BEAM COMMISSIONING OF AN SRF PLUG-GUN CAVITY PHOTOINJECTOR

M. Schmeißer*, R. Barday, A. Burrill, A. Jankowiak, T. Kamps, J. Knobloch,
O. Kugeler, P. Lauinger, A. N. Matveenko, A. Neumann, J. Völker, HZB, Germany
J. Sekutowicz, DESY, Germany; P. Kneisel, JLab, USA; J. Smedley, BNL, USA
R. Nietubyc, NCBJ, Poland; I. Will, MBI, Germany

Abstract

Superconducting rf photo-electron injectors (SRF photoinjectors) hold the promise to deliver high brightness, high average current electron beams for future light sources or other applications demanding continuous wave operation of an electron injector. This paper discusses results from beam commissioning of a hybrid SRF photoinjector based on a Pb coated plug and a Nb rf gun cavity for beam energies up to 2.5 MeV at Helmholtz-Zentrum Berlin (HZB). Emittance measurements and transverse phase space characterization with solenoid-scan and slit-mask methods will be presented.

MOTIVATION

Next generation accelerator based light sources like Energy-Recovery Linac (ERL) driven synchrotron radiation sources, Free Electron Lasers, or THz radiation sources require electron beam injectors capable of delivering high brightness electron beams with short pulse length at high average current. The SRF photoinjector paradigm allows operation at high beam loading with low rf power dissipation. Thus, continuous wave (CW) operation and acceleration of a high average power, high brightness beam is possible. The aim of this project is the generation of and measurements with an electron beam from an SRF photoinjector based on a hybrid Nb/Pb gun cavity [1]. We seek to further our understanding of implications arising from the presence of a cathode film in the gun cavity on the performance of the cavity itself and the electron beam generated and accelerated with the gun. The work could lead to a suitable concept for an electron source driving an FEL/THz class CW linear accelerator.

PERFORMANCE SUMMARY

The experiments have been carried out at GunLab, the injector test facility of BERLinPro [2] at HZB. Two versions of gun rf cavities have been tested with beam. The cold mass (SRF cavity, coupler and solenoid magnet) of the SRF photoinjector [3] was built to fit inside the HoBiCaT [4] cryomodule at HZB. A photocathode drive laser for UV light, developed by MBI, and a diagnostics beamline [5] complete the facility, enabling us to measure electron beam properties [6], cathode performance with regard

to quantum efficiency and dark current [7], and rf aspects of the SRF cavity [8, 9].

Two Nb rf cavities, cavity 0.1 and cavity 0.2, with 1.6 cells and an accelerating mode at 1.3 GHz have been designed by DESY and HZB, built by JLab [10], and tested with the setup at HZB. The cathode film for both cavities was applied by means of filtered cathodic arc deposition at NCBJ [11]. For cavity 0.1, the Pb cathode film was applied directly to the inside back wall of the first cavity half-cell, for cavity 0.2 the Pb cathode film was deposited on a Nb plug, which can be inserted through the back of the cavity half-cell. The Nb plug is vacuum sealed with an Indium gasket allowing good thermal and electrical contact between plug and cavity. The advantage of the plug design is the possibility to change the photocathode and to test different deposition techniques with the same cavity. Furthermore, the plug concept allows decoupling of the cavity treatment from the cathode deposition.

Typical setup and beam parameters obtained during runs with both cavities in 2011 and 2012 are summarized in Table 1. Both cavities reached field gradients of 35 MV/m

Table 1: Typical setup and beam parameters measured running at 8 kHz repetition rate and illumination of the cathode with 2.5 ps long (fwhm) laser pulses at 258 nm.

Parameter	Gun 0.1	Gun 0.2
Cathode material	Pb on wall	Pb on plug
Cathode QE_{\max} at 4.8 eV	$1 \cdot 10^{-4}$	$1 \cdot 10^{-5}$
Electric peak field	20 MV/m	27 MV/m
Launch field at emission	5 MV/m	7 MV/m
Beam kinetic energy	1.8 MeV	2.5 MeV
Bunch charge	6 pC	187 fC
Bunch emission time (rms)	2...4 ps	2.5...3 ps
Average current	50 nA	1.5 nA
Norm. emittance per mm laser spot size	5.4 mm mrad	1.9 mm mrad

in the vertical test area (VTA) at JLab. During operation at HoBiCaT, the field gradient was limited by field emission followed by slow quench to 20 MV/m for cavity 0.1 and 28 MV/m for cavity 0.2 [9]. The launch field during emission is the peak field multiplied with the sine of the launch phase at which the electrons gain maximum energy during passage of the cavity. For the 1.6 cell cavity design and at gradients in the 20 to 30 MV/m range the launch phase for maximum energy gain is 10 to 15 deg of the rf.

* martin.schmeisser@helmholtz-berlin.de

The requirement of a high peak field could be mitigated by a 1.4 cell design with an inclined back wall. As shown in beam dynamics studies, it exhibits higher launch fields for given peak field and thus an improved emittance performance [12, 13]. The QE for cavity 0.1 is higher than for cavity 0.2 by a factor of 10 because laser cleaning with an excimer laser of the Pb cathode film was only performed with cavity 0.1 [7]. Lower average drive laser power further reduced the average current generated from the cathode by a factor of 3. The field emission threshold was higher and the extracted dark current was lower for cavity 0.2 [7]. This can be attributed to a smoother Pb film surface with less protrusions and droplets. This shows that preparation of the cathode film on a plug is superior to direct preparation on the inner surface of the cavity back plane. This is due to the fact that the deposition source can be placed closer to the substrate, minimizing the distance over which droplets are formed. Another indication for improvement is the scaling of the transverse normalized emittance with laser spot size. For cavity 0.1, we found a strong scaling with 5.4 mm mrad per mm laser spot size. We found that protrusions and droplets on the cathode surface cause regions with strong radial electric fields leading to heating up of the transverse emittance [6]. For cavity 0.2, the slope is smaller, about 1.9 mm mrad per mm laser spot size. In order to study this with more detail, we improved the diagnostics beamline enabling us to perform phase space measurements.

SETUP AND PROCEDURES

GunLab Electron Beamline

A schematic overview of the diagnostics beamline is shown in Fig. 1. The beamline is equipped with several YAG:Ce viewscreens, a slit mask and a spectrometer dipole. The screens are imaged at a 45 deg angle by CCD cameras. Copper Faraday cups are used for current measurements and as beam dumps. A Tungsten plate with

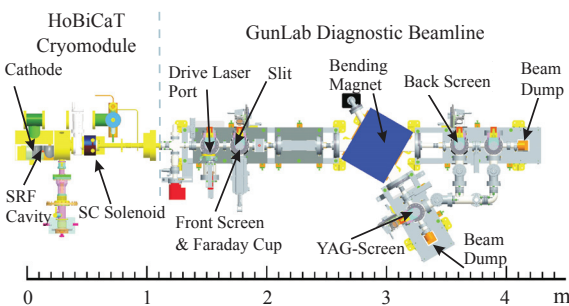


Figure 1: HoBiCaT cryomodule and GunLab beamline.

1.5 mm thickness and a 0.1 mm slit aperture allows phase space measurements. The screens at the slit station and in the dispersive section were coated with a thin Indium Tin Oxide (ITO) layer for charge transport to avoid damage of the crystals due to charging up effects from low energy electrons stopped in the screen material [14].

Measurement Procedures

Three individual measurements were conducted to characterize the phase space of one beam setting. First, the beam was imaged on the front screen without slit to calibrate the steerer angle and vertical offset. In a second sweep the front screen was used again, but with the slit to measure the beamlet intensity. Finally, the beamlets were allowed to drift towards the back screen in order to measure the divergence of each beamlet. All measured values were taken from ten polls per beamlet on the back screen and five polls per beamlet on the front screen. Mean and standard deviation were recorded. The phase space distributions were corrected for the steerer angle and summed up to obtain second moments and the emittance as described in [15].

In order to conduct a solenoid scan, the current in the solenoid was varied over a specified range. Screen images were saved for a single poll per solenoid setting, while beam positions and diameters were averaged over six polls. Beam parameters and the emittance are obtained from a quadratic fit of the beam width against the inverse focal length of the solenoid.

EXPERIMENTAL RESULTS

Phase Space Emittance vs. Laser Spot Size

The vertical phase space was characterized with the slit mask for different laser spot sizes with a rf cavity gradient of 10 MV/m at an emission phase of approximately 15 deg. For comparison the emittance measurement was repeated using the solenoid scan. A round aperture in the laser beam line was used to manipulate the laser spot size, however, other laser settings remained constant so the bunch charges were not equalized among the measurements (but all below the space charge regime). The resulting emittance values are displayed in Fig. 2. A linear dependency of the

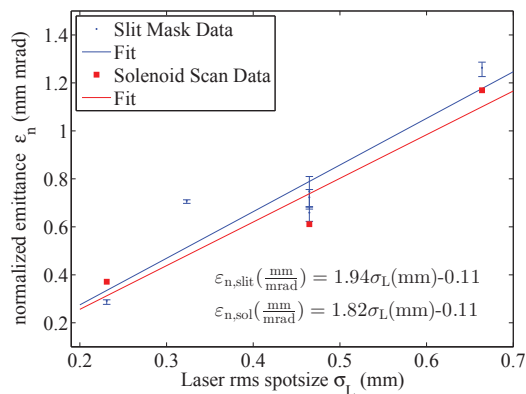


Figure 2: Results of emittance measurements.

normalized emittance with respect to the rms laser spot size can be recognized, despite the scattering of the data. The corresponding phase spaces are displayed in Fig. 3, where at large spot sizes a structured phase space was obtained. This hints at structured emission from hot spots on

the cathode surface which may be covered with protrusions and droplets. Yet, the lower emittance implies an improved surface quality over the coating in cavity 0.1.

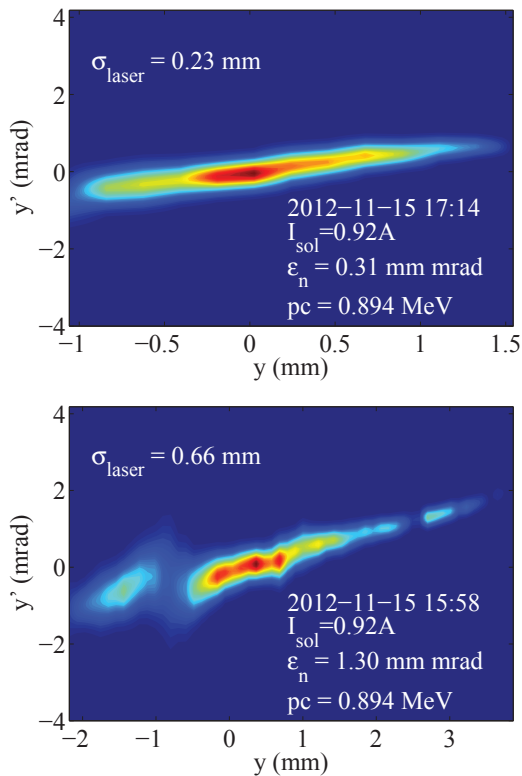


Figure 3: Reconstructions of vertical phase spaces.

Uncertainties due to temporal deviations and other statistical errors are estimated to amount to less than 5%. The finite size of the YAG screen together with a 45 deg viewing angle may introduce an overestimation of the measured beam size of up to $30 \mu\text{m}$ [14]. From a numerical estimate this will introduce a systematic error of about +3% in the emittance. Only these effects are taken into account by the error bars in Fig. 2. Space charge effects are negligible at the observed bunch charges below 1 pC and the short pulse length of 2.5 to 3 ps minimizes the rf contribution to the emittance. The accuracy of the evaluated emittance is largely defined by the dynamic range of the entire measurement, which differs between measurements because beamlets at the tail of the distribution might move off the screen due to geometrical constraints. The range differs between 2.5 and 6.4 dB, which implies that differences as large as 20% in the number of considered particles occur.

Energy Phase Scan Results

The dispersive arm of the beamline was used to determine the phase dependence of the beam kinetic energy at different cavity gradients. For low gradients, the momentum decreases with the launch phase. At the peak gradient of 27 MV/m, the energy shows a shallow maximum at about 15 deg.

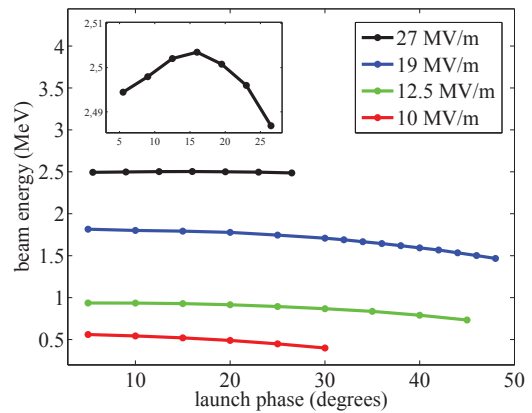


Figure 4: Results of beam energy measurements at different field gradients.

SUMMARY AND OUTLOOK

The beam performance capabilities of an SRF photoinjector based on the hybrid Nb/Pb plug-gun cavity have been studied experimentally. The plug-gun concept offers advantages over the direct coating of the inner back wall. Lower dark current and lower emittance offer high performance characteristics for the hybrid Nb/Pb gun. Future R&D efforts should be directed to improve the compatibility of cathode deposition and SRF cavity treatment and to develop pre- and in-situ cleaning procedures for the cathode film.

ACKNOWLEDGMENTS

The authors would like to thank all colleagues at HZB, DESY, JLAB, MBI, BNL and NCBJ involved in the Pb/Nb gun cavity project. The work at HZB is supported by BMBF and the State of Berlin.

The Pb deposition activity at DESY and NCBJ and the beam time at HZB is supported by EuCARD.

REFERENCES

- [1] J. Sekutowicz, *et al.*, PRST-AB 8, 010701 (2005).
- [2] A. Jankowiak, *et al.*, Proc. of LINAC 2010, TUP007, p. 407.
- [3] T. Kamps, *et al.*, Proc. of IPAC 2011, THPC109, p. 3143.
- [4] O. Kugeler, *et al.*, RSI 81, 074701 (2010).
- [5] R. Barday, *et al.*, Proc. of DIPAC 2011, TUPD007, p. 317.
- [6] J. Voelker, *et al.*, Proc. of IPAC 2012, TUPPD051, p. 1518.
- [7] R. Barday, *et al.*, Proc. of IPAC 2013, MOPFI001.
- [8] A. Neumann, *et al.*, Proc. of IPAC 2011, MOODA03, p. 41.
- [9] A. Burrill, *et al.*, Proc. of IPAC 2013, WEPWO002.
- [10] P. Kneisel, *et al.*, Proc. of PAC 2009, TU5PFP053, p. 945.
- [11] R. Nietubyc, *et al.*, Proc. of IPAC 2010, THPEC020, p. 4086.
- [12] A. Neumann, *et al.*, Proc. of IPAC 2013, MOPFI003.
- [13] T. Kamps, *et al.*, Proc. of LINAC 2012, THPB069.
- [14] R. Barday, *et al.*, Proc. of IBIC 2012, MOPB73.
- [15] S.G. Anderson, *et al.*, PRST-AB 5, 014201 (2002).